Interaction between magnetic and structural ordering in DyH_{2+x}

P. Vajda* and J. N. Daou
Hydrogène dans les Métaux, Bâtiment 350, Université Paris–Sud, F-91405 Orsay, France
(Received 10 October 1991)

The electrical resistivity of DyH_{2+x}, with $0 \leq x \leq 0.27$, was measured in the temperature range $1.4 \leq T \leq 300$ K. The data indicate short- and long-range structural ordering in the excess hydrogen (x) sublattice: short range near 150 K for $0.05 \lesssim x \lesssim 0.10$, and long range between 150 and 250 K, for $x > 0.10$. Quenching across the anomaly introduced defects in the ordered x sublattice (probably isolated H atoms on octahedral sites) resulting in a resistivity increase, $\Delta\rho_q$. The recovery analysis of $\Delta\rho_q$ permitted a determination of the activation energy of the migrating species: $E_a = 0.16(1)$ eV for the short-range-ordered (SRO) configuration and 0.14(1) eV for the long-range-ordered (LRO) configuration. Magnetic transitions were observed at $T_I = 5.1(1)$ K and $T_N = 3.3(1)$ K for $x = 0$; with increasing x, the magnetic manifestations diminish and vanish completely for $0.05 < x < 0.13$, giving rise at the same time to a resistivity minimum at $6 \lesssim T_m \lesssim 16$ K. Above $x = 0.13$ an additional λ-type magnetic transition appears at $T = 10.7$ K, strongly suppressed in the quenched specimens, which is probably induced by the LRO configuration of the x sublattice.

I. INTRODUCTION

Like the great majority of the other rare-earth dihydrides, DyH_2 is metallic and crystallizes in the fcc fluorite-type β phase, with ideally both tetrahedral (T) sites occupied. Additional x hydrogen atoms enter the octahedral (O) sites, to give the superstoichiometric dihydride, DyH_{2+x}. The limiting concentration $x^{\beta}_{\max}$, before transforming into the hexagonal trihydride (γ phase) depends on sample purity and its metallurgical state: For well-annealed 99.99% pure starting material, $x^{\beta}_{\max}$ is close to 0.25 at. % H/at. % Dy.[1] Similarly, the composition of the "pure" dihydride depends strongly on the sample preparation conditions and can vary between $DyH_{1.83}$ and $DyH_{1.99}$.

The magnetic properties of the pure dihydride have been studied by susceptibility,[2,3] specific heat,[4] and Mössbauer-effect[5,6] measurements. In general, two magnetic transitions were observed at temperatures varying from one experiment to another, the most reliable ones being 3.3(2) and 5.0(5) K. The difficulty to obtain reproducible results is obviously related to a badly defined stoichiometry, especially in older work, and we shall see later how the various discrepancies can be accounted for. Neutron-diffraction work on DyD_2 (Ref. 7) has been used to specify the magnetic structures: Below $T_N \approx 3.5$ K, the spins order antiferromagnetically (AF) in a commensurate structure modulated with a period of $4a_0/\sqrt{11}$ along [113], while between T_N and $T_I \approx 5$ K, an intermediate AF structure appears, whose details have not been established yet except that it is incommensurate with the lattice. Finally, the temperature dependence of the electrical resistivity was used (i) to determine the influence of the crystal field upon the magnetic (spin disorder) resistivity ρ_{mag} of several rare-earth dihydrides including DyH_2,[8] and (ii) to investigate the optical vibrations of the H sublattice and to determine its Einstein temperature.[9]

As concerns the superstoichiometric system DyH_{2+x}, no systematic studies had been undertaken until now to our knowledge, besides occasional measurements on ill-defined samples. Thus, Carlin and Krause's dihydride is given as $DyH_{2.04}$ (Ref. 3) and exhibits a broad maximum at 6 K, while Dunlap *et al.* report a transition temperature of about 20 K for $DyH_{2.14}$.[5] Finally, Shaked *et al.* did not observe any magnetic reflections on $DyD_{2.06}$ down to 1.4 K.[7]

In this paper, we present electrical resistivity measurements on the system DyH_{2+x}, with $0 \leq x \leq 0.27$, in the temperature range $1.4 \leq T \leq 300$ K. In particular, we report structural ordering in the octahedral x sublattice at $T_{an} \sim 150$–250 K for x values above ~ 0.05, which interacts strongly with the magnetic structures, in this resembling closely manifestations observed earlier on the systems SmH_{2+x},[10] GdH_{2+x},[11] and TbH_{2+x}.[12]

II. EXPERIMENT

The specimens were prepared from 99.99 at. % (as concerns metallic impurities), cold-rolled dysprosium foils of 200-μm thickness furnished by the Ames Laboratory (Ames, Iowa) with a stated impurity content of: main metallic impurities (>2 at. ppm)—18 Cu, 15 Fe, 8 Mn, 5.5 Cr, 5 Ta, 3 Na, 3 Tb, 3 Ho, and 2.5 W; gaseous impurities (at. ppm)—285 O, 180 F, 75 Cl, 40 C, 40 H, and 34 N. They were cut into $20 \times 1 \times 0.2$ mm^3 strips and provided with four spot-welded platinum leads for contacts. They were then loaded with hydrogen in two steps: (1) at 550–600 °C to give the "pure" dihydride, in our case $DyH_{1.97-1.99}$: and (2) at 300 °C to add the excess hydrogen atoms, x. The obtained specimens corresponded to $x = 0$ (twice), 0.02, 0.055, 0.074, 0.10, 0.13, "0.18," 0.22, and 0.27. [The specimen with $x =$ "0.18" exhibiting unusual behavior, we have degassed it after the run to check the concentration. The value of 0.18 at. %

H/at. % Dy was confirmed, but, contrary to other samples, it had released its x atoms in *two* steps (at 240 and at 300 °C), probably indicating the presence of some precipitated insulating γ-phase nuclei, leaving the sample with a smaller effective x value in the β phase, of the order of $x_\beta \sim 0.10$.]

The electric measurements were done in a pumped liquid-helium cryostat, using the classical dc four-point method; the sample holder permitting measurements of up to seven specimens at the same time, this guarantees a relative precision in the temperature determination of 0.01 K in the magnetically interesting region below ~20 K. Quench experiments were performed, in order to conserve the room-temperature configuration of the x-hydrogen atoms, by dipping the sample holder into liquid nitrogen, with a cooling rate of the order of 10^3 K/min, as compared to slowly cooled (or relaxed) samples with a rate of 0.3 K/min.

III. RESULTS AND DISCUSSION

The electrical resistivity can be written as a sum of several contributions:

$$\rho_{\text{tot}}(T)=\rho_r+\rho_{\text{mag}}(T)+\rho_{\text{ph}}(T)\ ,$$

where ρ_r is the residual resistivity; $\rho_{\text{mag}}(T)$ includes the paramagnetic spin disorder resistivity, which can be temperature dependent when $kT \sim \Delta E_{ij} \equiv \varepsilon_j - \varepsilon_i$ is of the order of a crystal-field (CF) level splitting; $\rho_{\text{ph}}(T)$ is the phononic resistivity including both acoustic and optical contributions (see, e.g., Ref. 9). As the observed phenomena, though not independent, occur in different temperature domains, we shall for the ease of the discussion separate the structural ordering from the magnetic one in the presentation of the results.

A. Structural ordering

Figure 1 shows the total resistivity through the whole measured temperature range for several selected DyH_{2+x} specimens with $0 \le x \le 0.13$. The residual resistivity of the pure dihydride is $\rho_r = 0.45\ \mu\Omega$ cm giving a resistivity ratio $\rho_{295}/\rho_r \approx 60$, a sign of its closeness to stoichiometry and the absence of structural defects, in particular of octahedral (x) hydrogen atoms within the limits of 0.001 at. % H/at. % Dy. The drop at low temperature is due to magnetic ordering and will be discussed later, while the apparently unorthodox behavior between 5 and ~150 K is caused by the crystal field and had been treated in detail in Ref. 8 for DyH_2. There, the CF-level scheme established from heat-capacity[4] and Mössbauer-effect[6] experiments using Γ_7 as ground state and $\Gamma_8^{(1)}$ and $\Gamma_8^{(2)}$ as the two first excited states, with $\Delta E_{21} \approx 100$ K and $\Delta E_{31} \approx 200$ K, gave a good fit to the experimental data. The linear part between 150 and 250 K gives a $d\rho/dT = 0.06\ \mu\Omega$ cm/K, close to the values obtained for the neighboring RH_2 systems,[10–12] indicating a similar electron-phonon coupling strength. The slight upward curvature above ~250 K is due to the start of scattering by the optical phonons.[9]

The $x = 0.02$ sample resistivity (Fig. 1) is just shifted by the increase of ρ_r due to introduction of interstitial H atoms on octahedral sites, giving a $\Delta\rho/\Delta x \approx 2$–$2.5\ \mu\Omega$ cm/at. % x atoms. From $x = 0.055$ on we note, however, the appearance of a break in the $\rho(T)$ curves in the region of 150 K, which is better seen in the differential representation of Fig. 2. The anomaly, whose maximum is situated at $T_{an} = 155$ K (independently of x up to 0.10), grows

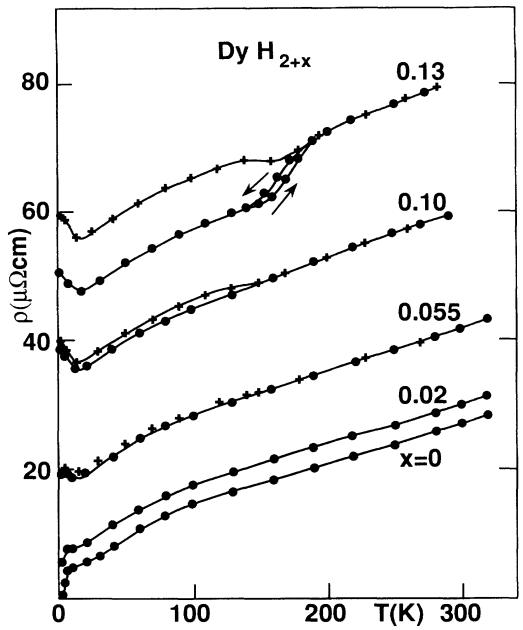

FIG. 1. Electrical resistivity as a function of temperature for DyH_{2+x}, with $x = 0$, 0.02, 0.055, 0.10, and 0.13. ●: in the relaxed state; +: after a quench from room temperature across the anomaly near 150 K. Note the hysteresis between 140 and 190 K for the $x = 0.13$ specimen.

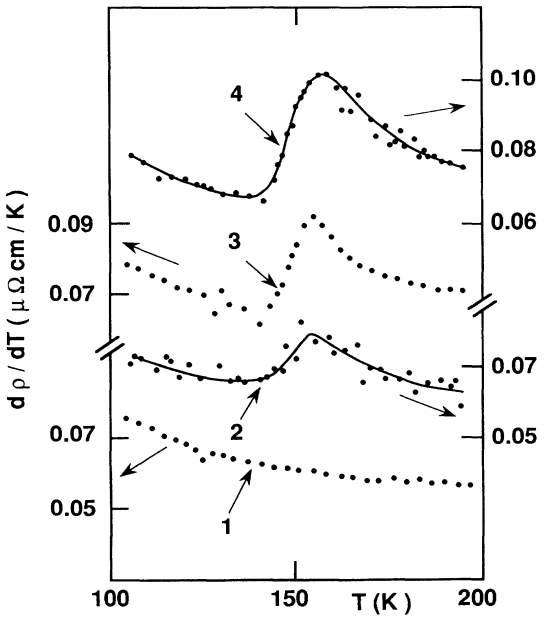

FIG. 2. Resistivity derivative in the anomaly region for various relaxed DyH_{2+x} specimens: 1, $x = 0$; 2, $x = 0.055$; 3, $x = 0.074$; 4, $x = 0.10$.

in amplitude with growing x resembling closely the anomalies observed for low x in other RH_{2+x} systems[10–13] and attributed to probable x-sublattice ordering in a short-range (SRO) configuration. For $x=0.13$, the anomaly becomes a real transition, the hysteresis indicating a probable first-order process at its origin. By analogy with other systems,[10–13] it is reasonable to suggest a long-range order (LRO) transformation in the octahedral sublattice as its driving mechanism.

A practical test for the proposed ordering phenomenon is a quenching experiment from a region above the anomaly (e.g., from room temperature) to one below it (liquid nitrogen). This should permit one to freeze in an eventual disordered state at low temperature (probably isolated H atoms on O sites), which should result in a resistivity increase. The crosses in Fig. 1 give the T dependence of the quenched sample resistivities, showing their annealing in the anomaly region. One can analyze the recovery process, assuming a first-order mechanism with a single activation energy E_a such that (see, e.g., Ref. 14)

$$E_a=-kT_p^2\left[\frac{d}{dT}\Delta\rho_q(T_p)\right]\Big/\Delta\rho_q(T_p)$$

can be directly obtained by measuring the quenched-in resistivity $\Delta\rho_q$ and its derivative at the peak temperature T_p of the annealing state. Figure 3 presents such an analysis for four samples with x between 0.05 and 0.13 (remember the remark concerning $x=$"0.18" in Sec. II). An interesting, though maybe not too surprising, result is the observation of two different peak temperatures T_p for the various samples: thus, for $x\leq 0.10$, we have $T_p=145$ K, while for $x=0.13$, $T_p=167$ K. The $x=$"0.18" specimen exhibits both peaks, being obviously in an intermediate situation and containing SRO and LRO regions; a rest of the SRO domains is probably still present in the form of a low-temperature asymmetry in the $x=0.13$ sample. The activation energies determined for the $x=0.05$ and $x=0.10$ specimens on one hand, and for the $x=0.13$ sample on the other, gave

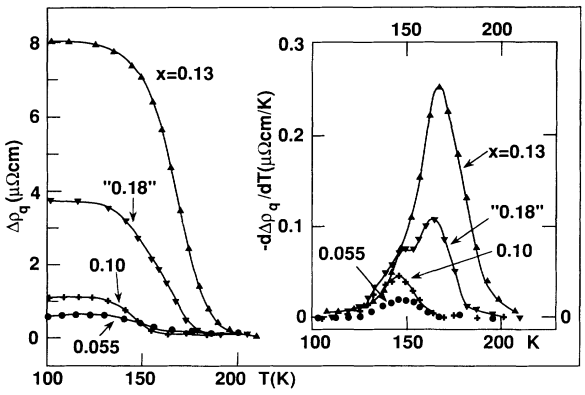

FIG. 3. Recovery of the quenched-in resistivity $\Delta\rho_q$ for various DyH_{2+x} specimens: ●, $x=0.055$; +, $x=0.10$; ▼, $x=$"0.18" (see text); ▲, $x=0.13$. Inset: derivative of the annealing curves for the above samples in the recovery region, used for the determination of the migration energies E_a (see text).

$$E_a^{\mathrm{SRO}}=0.16(1)\text{ ev}\quad\text{and}\quad E_a^{\mathrm{LRO}}=0.145(5)\text{ eV}\,.$$

The difference is at the limit of the error bars but plausible in view of the clearly different T_p's. The analysis of the $x=$"0.18" sample is not reliable due to the overlap of both processes.

Going over to the x-richest specimens, $x=0.22$ and 0.27 (Fig. 4), we note a distinct increase of the transformation region, both in temperature and in amplitude. This is particularly striking for the first specimen, where T_{an} (defined as the temperature of the slope maximum) is 260 K, the ordering region extending over nearly 100 K. Since the $x=0.27$ sample exhibits a slightly reduced anomaly, it is tempting to propose the optimal concentration for LRO somewhere near $x=0.25$, in view of the observed ordered structures driving tetragonal distortions in the metal lattice of CeH_{2+x} (Ref. 15) and CeD_{2+x} (Ref. 16) for similar x values. On the other hand, no structural change or distortion was observed on the metal lattice in DyH_{2+x} up to $x=0.27$ by x-ray diffractometry between 90 and 300 K,[1] which reminds us of analogous behavior in the system GdH_{2+x}.[11] The quenching has introduced a large resistivity increase $\Delta\rho_q$ in both samples, and we are presenting its recovery analysis in Fig. 5. The $x=0.22$ specimen exhibits clearly two recovery stages, one at $T_p\approx 155$ K, the other near 190 K with a tail toward higher temperatures. The activation energy of the first, sufficiently distinct stage was determined to $E_a(T_p=155\text{ K})=0.140(5)$ eV corresponding to the above determined E_a^{LRO}; its lower T_p is due to the smaller number of migrational jumps necessary for recombination in this higher-x sample. The recovery of the $x=0.27$ sample is complex, containing at least two overlapping processes between 160 and 180 K, and thus impossible to analyze correctly. The high-T recovery peaks at $T_p=180$–190 K are difficult to attribute without the de-

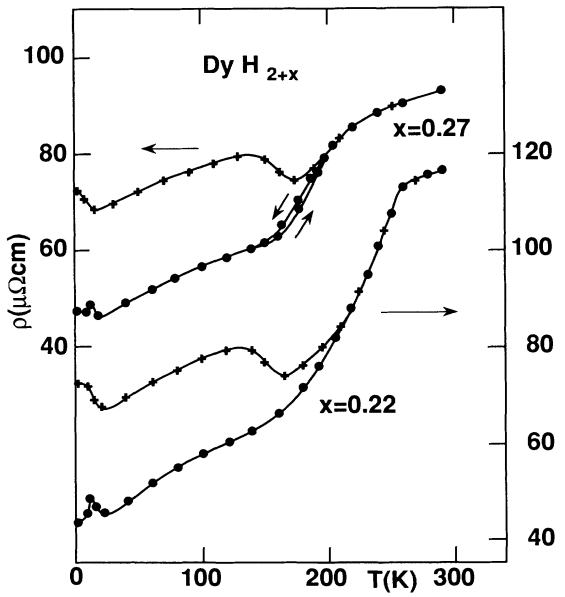

FIG. 4. Same as in Fig. 1, for $x=0.22$ and 0.27 in the relaxed (●) and in the quenched (+) state.

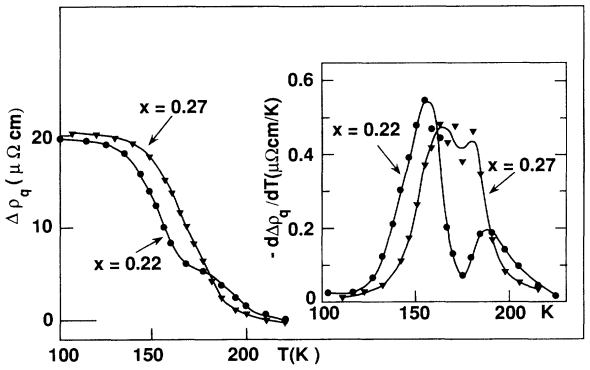

FIG. 5. Recovery of the quenched-in resistivity for DyH_{2+x}, with $x=0.22$ (●) and $x=0.27$ (▼). Inset: derivative of the annealing curves.

tailed knowledge of the ordered configurations in question, but could be due to some reorientational process. In any case, neutron-scattering work in progress should clarify the problems and specify the mechanisms at work.

B. Magnetic ordering

The electrical resistivity of the pure dihydride $DyH_{1.97}$ exhibits clear magnetic ordering below $T=5.1$ K, in good agreement with other experimental methods;[4–7] a second transition, with a change of slope, appears at 3.3 K. The inset in Fig. 6, representing the derivative $d\rho/dT$ in the magnetically ordered range, gives a good picture of the two transitions; moreover, it has a striking resemblance down to small details with the $c_p(T)$ dependence of Bieganski, Opyrchal, and Drulis.[4] This latter fact is very satisfactory, since the spin-wave scattering of the electrons in antiferromagnetics should give a temperature dependence for the respective magnetic contributions below T_N of the form $c_{mag} \propto T^3$ and $\rho_{mag} \propto T^4$. Now, Bieganski, Opyrchal, and Drulis[4] were able to fit their c_p data in the region 1.8–3 K such that c_{mag} (cal/mol K) $=3.19\times10^{-2}T^3$, while our measurements exhibit a very close to T^4 dependence, $\rho_{mag}(\mu\Omega$ cm$) =1.3\times10^{-2}T^{3.95}$, in the region 1.7–3.3 K (Fig. 7) for the intrinsic resistivity $\rho_{tot}-\rho_r$, which corresponds to ρ_{mag} in this T range with negligible ρ_{ph}. Thus, we are also confirming the "normal" commensurate antiferromagnetism below $T_N=3.3$ K and the less normal incommensurate AF between 3.3 K and $T_I=5.1$ K, as suggested by neutron diffraction[7] for the pure DyH_2.

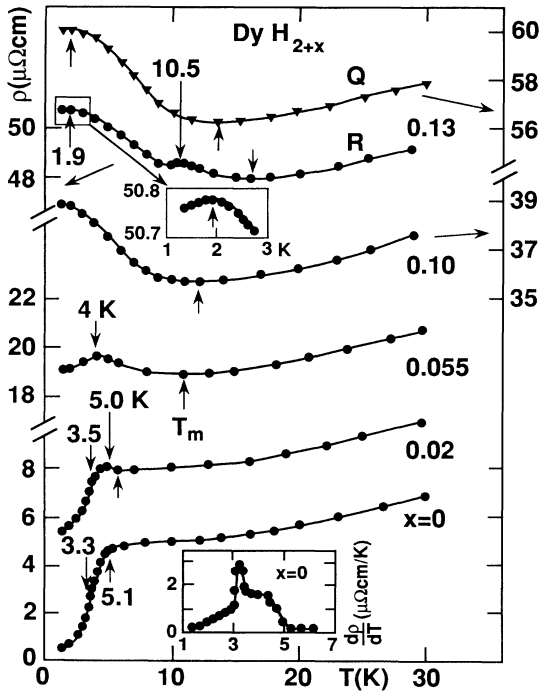

FIG. 6. Low-temperature resistivity of DyH_{2+x}, with $x=0$, 0.02, 0.055, 0.10, and 0.13 in the relaxed (R,●) and in the quenched (Q,▼) state, showing the magnetic transitions and the resistivity minima at T_m. Lower inset: derivative for the $x=0$ specimen in the magnetic region; upper inset: blow-up of the low-temperature maximum for $x=0.13$. Note the shifted ordinate scales.

With increasing x, the magnetic manifestations begin to wipe out: the transitions are rounded off and ρ^0_{mag} decreases: for $x=0.055$, there is only a small break left at $T_N\approx4$ K, while for $x=0.074$ (not shown) and $x=0.10$, no ρ decrease due to magnetic ordering is seen down to 1.4 K. On the other hand, a minimum in $\rho(T)$ begins to show up, increasing in amplitude and in position. The temperature of this minimum T_m grows from $T_m\approx5.5$ K for $x=0.02$ to 16 K for $x=0.13$. Its origin could be sought, similar to TbH_{2+x} (Ref. 12) and GdH_{2+x},[11] in an increase of the resistivity (with decreasing T) due to electron scattering by new magnetic superzone boundaries introduced by the incommensurate structure, such that, according to the Elliott-Wedgwood theory,[17] $\rho_{tot} \propto (1-\delta M)^{-1}$, where M is the magnetic order parameter and δ is related to the gap in the superzones. Another

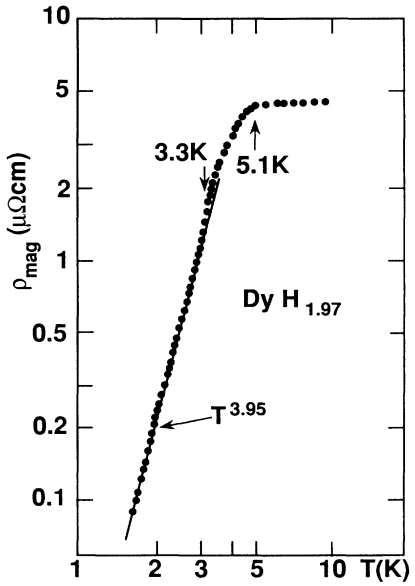

FIG. 7. Intrinsic resistivity, $\rho_{mag}=\rho_{tot}-\rho_r$, for the pure dihydride in a double-logarithmic plot to show the $T^{\sim4}$ dependence below $T_N=3.3$ K.

possibility is the appearance of magnetic fluctuations due to short-range ordering extending beyond T_N or T_I. This point should be clarified by further neutron-diffraction work.

The richest x specimen in Fig. 6, $x=0.13$, begins to exhibit a new feature, namely a bump at 10.5 K, and a small but definite maximum at 1.9 K (see also the upper inset). The bump disappears again in the quenched sample. The reality of its existence (we had first suspected some spurious effects) is beautifully confirmed by the relaxed $x=0.22$ sample shown in Fig. 8. There, the minimum has shifted to $T_m=20.5$ K, and a striking λ-like feature shows up, with a maximum at 10.7 K, just at the position of the bump for $x=0.13$. The strong drop at 10 K is followed by a slower decrease of the form $\rho_{\rm mag} \propto T^2$, which is the classical temperature dependence given by the spin-wave spectrum of a ferromagnet without anisotropy (see, e.g., Ref. 18). The quench again modifies strongly the magnetic manifestations: the 10.7-K peak shows up just as a small shoulder near 9 K superimposed upon a growing $\rho(T)$ dependence up to a complex maximum near 4 K (see inset). The richest $x=0.27$ specimen, seems to exhibit a mixture of the $x=0.13$ and 0.22 features: a somewhat smaller but still very clear 10.7-K peak and a small maximum at 2.5 K; the quench eliminates the 10.7-K structure completely.

From what is discussed above, it is clear that the high-temperature ordering of the hydrogen sublattice, with its maximum effect for $x=0.22$, is responsible for the appearance of the 10.7-K magnetic transition. The nonexistence of the latter for $x<0.13$ and, in particular, its partial or complete vanishing after a quench from room temperature, is a strong indication that the presence of a LRO structure in the x sublattice is a necessary condition for its appearance. A lowering of the CF symmetry from cubic in the case of DyH_2, with pure T-site occupation, to possibly tetragonal in the case of an ordered octahedral H sublattice [cf. also CeH_{2+x} (Refs. 15 and 16)], or axial such as was suggested for some TbH_{2+x} samples by Drulis, Opyrchal, and Borkowska[19] could modify the level structure sufficiently to lead to new magnetic ordering transitions. A more profound modification of the electronic structure, e.g., of the Fermi surface, is not excluded either, in view of the results for GdH_{2+x},[11] where similar interactions between magnetic and structural ordering could not be attributed to CF effects because of the latter's negligible influence.

In addition, our data in Figs. 6 and 8 permit a more precise assignment of the few DyH_{2+x} experiments reported in the literature. Thus, Carlin and Krause's[3] "dihydride," given as $DyH_{2.04}$, with a single broad susceptibility maximum near 6 K, would correspond to our $x=0.055$ specimen. The $DyD_{2.06}$ sample of Shaked *et al.*,[7] which did not show magnetic reflections down to 1.4 K, behaves like our $x=0.074$ and 0.10 specimens; this is very satisfactory as their "pure" dihydride was

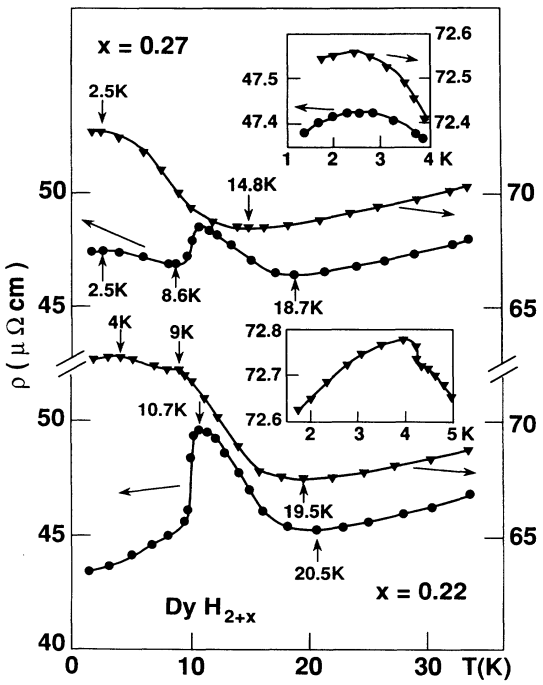

FIG. 8. Low-temperature resistivity of DyH_{2+x} with $x=0.22$ and 0.27 in the relaxed (●) and in the quenched (▼) state, indicating the magnetic transition and the minima. The insets show a blow-up of the low-temperature maxima.

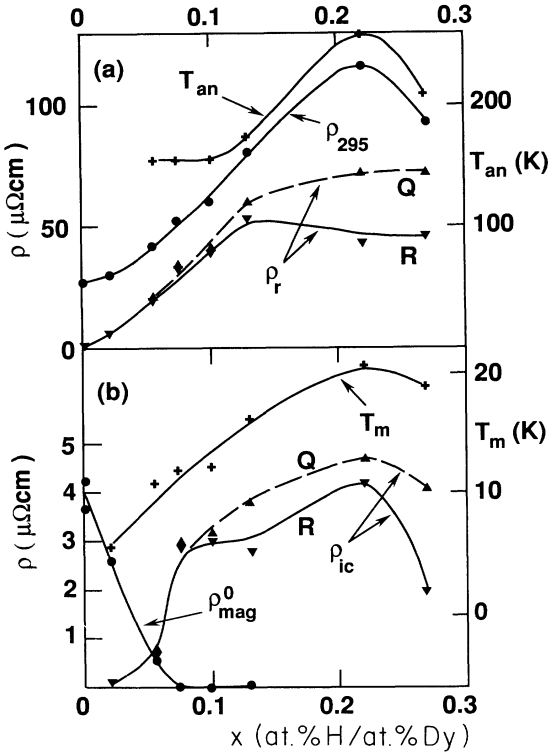

FIG. 9. Various characteristic parameters as a function of the excess hydrogen concentration x. (a) Residual resistivity ρ_r in the relaxed (R,▼) and in the quenched (Q,▲) state; room-temperature resistivity ρ_{295} (●); structural-anomaly temperature T_{an} (+). (b) Magnetic resistivity at T_N, $\rho^0_{\rm mag}$ (●); incommensurate resistivity, $\rho_{ic}=\rho(T_{\rm max})-\rho(T_m)$, in the relaxed (▼,$R$) and in the quenched (▲,Q) state; resistivity minimum temperature T_m (+).

close to $DyD_{1.96}$. Finally, the Mössbauer measurements on $DyH_{2.14}$,[5] indicating magnetic ordering below about 20 K, could mean that our $T_m = 20.5$ K for $x = 0.22$ corresponds to their transition temperature. But nowhere, to our knowledge, is there any mention of the 10.7-K transition.

IV. CONCLUDING REMARKS

As a kind of summary, we have plotted in Fig. 9 the x dependence of various characteristic parameters extracted from our experimental data. In the upper part, we are presenting the resistivities ρ_r and $\rho_{295\,K}$ as well as the structural anomaly temperature T_{an} showing the absence of LRO up to just below $x = 0.13$ (maximum of ρ_r for the relaxed specimens and beginning increase of T_{an}). The destruction of LRO at room temperature or by a quench leads to a steady increase of $\rho_r(Q)$ and of ρ_{295}, at least up to $x = 0.22$. (The small decrease for $x = 0.27$ could be a witness of a local precipitation of some γ phase.)

In the lower part of Fig. 9, we have collected the values for $\rho^0_{mag} = \rho(T_N) - \rho_r$, $\rho_{ic} = \rho(T_{max}) - \rho(T_m)$, as well as the minimum temperature T_m itself. The progressive disappearance of magnetic order for lower x values is signalized by the decrease of ρ^0_{mag} and is accompanied by the growing importance of the resistivity minimum; ρ_{ic} has a plateau around $x = 0.13$ in the relaxed specimens (corresponding to the ρ_r maximum in the upper part of the figure) which disappears upon freezing-in of the high-T disorder through quench. The same remark concerning the possible γ-domain precipitation for the $x = 0.27$ sample as above is to be applied here.

Concluding, we have shown the close interaction of the complex magnetic manifestations in DyH_{2+x} below ~ 20 K with the SRO in the hydrogen sublattice, which appears above $x \sim 0.05$ and turns into LRO above $x \sim 0.13$. The exact nature of the magnetic and structural configurations is to be determined through neutron-scattering experiments in progress.

Hydrogène dans les Métaux is part of the Laboratoire de Spectroscopie Atomique et Ionique du CNSR.

*Also at: Laboratoire des Solides Irradiés, Ecole Polytechnique, F-91128 Palaiseau, France.

[1]M. Chiheb, J. N. Daou, and P. Vajda (unpublished).
[2]Y. Kubota and W. E. Wallace, J. Chem. Phys. **39**, 1285 (1963).
[3]R. L. Carlin and L. J. Krause, Chem. Phys. Lett. **82**, 323 (1981).
[4]Z. Bieganski, J. Opyrchal, and M. Drulis, Phys. Status Solidi A **28**, 217 (1975).
[5]B. D. Dunlap, G. K. Shenoy, J. M. Friedt, and D. G. Westlake, J. Phys. (Paris) Colloq. **40**, C5-211 (1979).
[6]J. M. Friedt, G. K. Shenoy, B. D. Dunlap, D. G. Westlake, and A. T. Aldred, Phys. Rev. B **20**, 251 (1979).
[7]H. Shaked, D. G. Westlake, J. Faber, and M. H. Mueller, Phys. Rev. B **30**, 328 (1984).
[8]J. N. Daou, P. Vajda, and J. P. Burger, Phys. Rev. B **37**, 5236 (1988).
[9]J. P. Burger, J. N. Daou, and P. Vajda, J. Less-Common Met. **103**, 381 (1984).
[10]P. Vajda, J. N. Daou, and J. P. Burger, Phys. Rev. B **40**, 500 (1989).
[11]P. Vajda, J. N. Daou, and J. P. Burger, J. Less-Common Met. **172**, 271 (1991).
[12]P. Vajda, J. N. Daou, and J. P. Burger, Phys. Rev. B **36**, 8669 (1987).
[13]P. Vajda, J. N. Daou, J. P. Burger, and A. Lucasson, Phys. Rev. B **31**, 6900 (1985).
[14]J. N. Daou, P. Vajda, J. P. Burger, and A. Lucasson, Phys. Status Solidi A **98**, 183 (1986).
[15]E. Boroch and E. Kaldis, Inorg. Chim. Acta **140**, 89 (1987).
[16]J. Schefer, P. Fischer, J. Hälg, J. Osterwalder, L. Schlapbach, and J. D. Jorgensen, J. Phys. C **17**, 1575 (1984).
[17]R. J. Elliott and F. A. Wedgwood, Proc. Phys. Soc. London **81**, 846 (1963).
[18]B. Coqblin, *The Electronic Structure of Rare Earth Metals and Alloys* (Academic, New York, 1977).
[19]M. Drulis, J. Opyrchal, and W. Borkowska, J. Less-Common Met. **101**, 211 (1984).